Discrete-Time Wavelet Extrema Representation: Design and Consistent Reconstruction

Zoran Cvetković and Martin Vetterli, *Senior Member, IEEE*

***Abstract*—This paper studies wavelet transform extrema and zero-crossings representations within the framework of convex representations in $\ell^2(\mathbf{Z})$. Wavelet zero-crossings representation of two-dimensional signals is introduced as a convex multiscale edge representation as well. One appealing property of convex representations is that the reconstruction problem can be solved, at least theoretically, using the method of alternating projections onto convex sets. It turns out that in the case of the wavelet extrema and wavelet zero-crossings representations this method yields simple and practical reconstruction algorithms. Nonsubsampled filter banks that implement the wavelet transform for the two representations are also studied in this paper. Relevant classes of nonsubsampled perfect reconstruction FIR filter banks are characterized. This characterization gives a broad class of wavelets for the representations which are derived from those of the filter banks which satisfy a regularity condition.**

I. Introduction

WAVELET modulus maxima and wavelet zero-crossings representations [1], [2] are based on irregular sampling of the multiscale wavelet transform at points which have some physical significance. Modulus maxima and zero-crossings of the wavelet transform, in the case of continuous-time signals, provide information on singularities, which are considered to be among the most meaningful features for signal characterization. Besides, unlike regular sampling, such a sampling strategy attains shift invariance of the representation, and thus overcomes one of the major drawbacks of the wavelet series expansion. This was one of the main reasons for introduction of the two representations by Mallat *et al.* [1], [2], and their promising performances were demonstrated in applications to signal denoising and compression.

Although these representations stem from underlying continuous-time theory, implementation takes place in the discrete-time domain. Berman *et al.* [3] were the first to pose the problem in purely discrete-time, arguing that the discrete framework is the model of an actual implementation, and showing that wavelet transform extrema/zero-crossings provide stable representations of finite length discrete-time signals. However, a complete discrete-time framework for the two representations has not been developed yet. In this paper, we give rigorous analysis of several aspects of wavelet extrema and zero-crossings representations in $\ell^2(\mathbf{Z})$, in particular: implementation, wavelet design and reconstruction.

Wavelet modulus maxima or zero-crossings based signal processing schemes are implemented by nonsubsampled octave band filter banks. We investigate properties of such filter banks and give a complete characterization of finite impulse response (FIR) filter banks for wavelet modulus maxima and wavelet zero-crossings representations. Wavelets for the two representations can be derived from the filter banks using the procedure proposed by Daubechies [16], [14] for generating orthonormal bases from critically sampled filter banks. However, nonsubsampled filter banks being less constrained allows for the design of a broader class of wavelets. This point is illustrated by a design procedure for highly regular wavelets with a given number of vanishing moments.

Reconstruction algorithms proposed in this paper are based on alternating projections onto convex sets and converge to a *consistent estimate* of the original signal. The notion of *consistent estimate*, originally introduced by Thao and Vetterli [6], denotes a signal which has the same representation as the original. The set of consistent estimates, called *reconstruction set*, in the case of nonunique representations generally consists of more than a single signal. Although experiments in reconstruction from wavelet modulus maxima and wavelet zero-crossings representations [1], [2], [7] yielded very good results, it was shown by Berman [4] and Meyer [5] that these representation do not provide a unique characterization of signals in $\mathbf{R}^n$ and $L^2(\mathbf{R})$, respectively. That means that some information is lost when going to the representation domain. The reason we insist on the consistent reconstruction is because it means reconstruction without loss of information, that is, fully utilizing the information which is embedded in the representation. In other words, although in the nonunique case we are not able to achieve perfect reconstruction, a consistent reconstruction algorithm yields a signal which at least has all of the properties of the original signal as described by the representation. A problem with wavelet modulus maxima representation is that it is nonconvex, which makes the reconstruction difficult. Hence, in this paper we study the wavelet extrema representation, which is a convex variant of the wavelet modulus maxima scheme, and propose simple and efficient algorithms for consistent reconstruction from wavelet transform extrema or zero-crossings. Numerical complexity of the proposed algorithms is $O(JN)$ operations per iteration

Manuscript received October 6, 1993; revised August 18, 1994. This work was supported by the National Science Foundation under Grants ECD-88-11111 and MIP-90-14189. This work was presented in part at the Annual CISS, Baltimore, MD, March 1993 and ICASSP'94, Adelaide, Australia. The associate editor coordinating the review of this paper and approving it for publication was Prof. Roberto H. Bamberger.

The authors were with the Department of Electrical Engineering and the Center for Telecommunications Research, Columbia University, NY, New York 10027–6699 USA. They are now with the Department of Electrical Engineering and Computer Science, University of California at Berkeley, Berkeley, CA 94720 USA.

IEEE Log Number 9408230.

for signals of length N and wavelet transform across J scales.

For similar reasons, in the case of two-dimensional signals we propose wavelet zero-crossings representation as a convex alternative to the wavelet modulus maxima representation. The wavelet modulus maxima representation for two-dimensional signals was proposed by Mallat *et al.* [2], [7] as a tool for extracting information on multiscale edges. For a particular class of the wavelet transform analysis filters, zero-crossings of the wavelet transform also occur at points of sharp image variations. As a consequence of the convexity, it is possible to achieve consistent reconstruction with a simple iterative algorithm. As an illustration, we report results of image reconstruction using this new algorithm.

The outline of the paper is as follows. Section II introduces definitions of the wavelet extrema and wavelet zero-crossings representations and establishes their relation. Relevant properties of nonsubsampled filter banks and the design of wavelets are studied in Section III. Algorithms for consistent reconstruction are described in Section IV, which also introduces the wavelet zero-crossings representation of two-dimensional signals. Results of experiments in signal reconstruction from the two representations are reported in Section V.

Notations: For a real discrete-time filter $H(z)$, let $\tilde{H}(z)$ denote the filter whose impulse response is the time-reversed version of the impulse response of $H(z)$. The Fourier transform of $\phi(x) \in L^2(\mathbf{R})$ will be written as $\hat{\phi}(\omega)$. For the dilated and scaled version of $\psi(x)$, the notation $\psi_s(x) = \frac{1}{s}\psi(\frac{x}{s})$ will be used. Convolution of functions in $L^2(\mathbf{R})$ will be denoted by $*$: $f * g(x) = \int_{-\infty}^{+\infty} f(u)g(x-u)du$.

II. Wavelet Extrema and Wavelet Zero-Crossings Representations: Definitions and Mutual Relationship

Wavelet extrema and zero-crossings representations are considered here in the discrete-time domain, for signals in $\ell^2(\mathbf{Z})$. The wavelet transform will refer to the bounded linear operator $\mathbf{W}: \ell^2(\mathbf{Z}) \to \ell^2(\mathbf{I})$, where $\ell^2(\mathbf{I}) = \ell^2(\{1, 2, \cdots, J+1\} \times \mathbf{Z})$, consisting of $J+1$ linear operators $W_j: \ell^2(\mathbf{Z}) \to \ell^2(\mathbf{Z})$, $j = 1, 2, \cdots, J+1$. The operators W_j are the convolution operators with the impulse responses of filters

$$\begin{aligned} V_1(z) &= H_1(z), \\ V_2(z) &= H_0(z)H_1(z^2), \\ &\cdots \\ V_J(z) &= H_0(z)\cdots H_0(z^{2^{J-2}})H_1(z^{2^{J-1}}), \\ V_{J+1}(z) &= H_0(z)\cdots H_0(z^{2^{J-2}})H_0(z^{2^{J-1}}) \end{aligned}$$

respectively. This is the type of transform implemented by an octave band nonsubsampled filter bank with analysis filters $H_0(z)$ and $H_1(z)$, as shown in Fig. 1(a) for $J = 4$. FIR nonsubsampled octave band filter banks are studied in more detail in Section III. In the following, signals in $\ell^2(\mathbf{Z})$ will be denoted by lower case letters, $f, g, \ldots$ and their wavelet transforms by corresponding upper case letters, $F = \mathbf{W}f, G = \mathbf{W}g, \ldots$. Any vector F in $\ell^2(\mathbf{I})$ will represent a $(J+1)$-tuple of vectors in $\ell^2(\mathbf{Z})$, $F = (F^1, F^2, \cdots, F^{J+1})$, so a jth octave band component of $\mathbf{W}f$ will be denoted by $W_j f = F^j$.

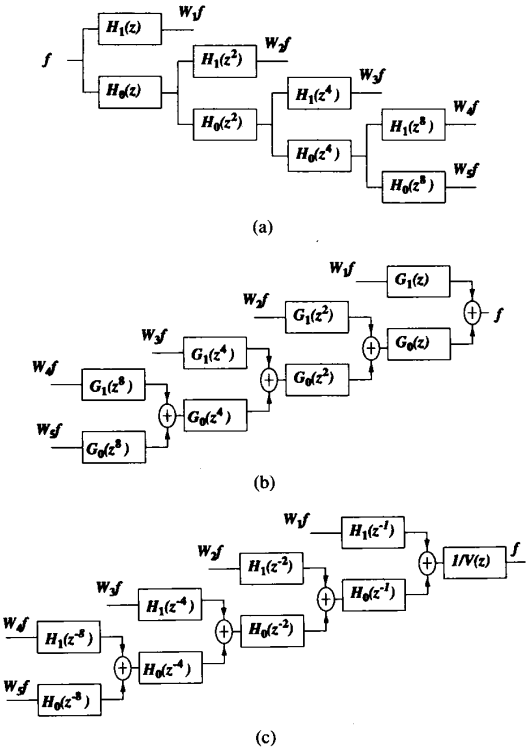

Fig. 1. Wavelet transform: (a) Filter bank implementation of the $\mathbf{W}$ operator; (b) filter bank implementation of an inverse of $\mathbf{W}$; (c) filter bank implementation of the $\mathbf{W}^*$ operator.

The definitions of the wavelet extrema and zero-crossings representations adopted here are essentially those introduced by Berman *et al.* [3]. In the following, M_a and M_i will denote the operators which give the locations of local maxima and minima respectively of some signal f,

$$M_a f = \{k: f(k+1) \le f(k),\ f(k-1) \le f(k)\}, \quad (1)$$

$$M_i f = \{k: f(k+1) \ge f(k),\ f(k-1) \ge f(k)\} \quad (2)$$

while M will stand for the operator extracting values of some signal at its local extrema points

$$Mf = \left\{f(k),\ k \in M_a f \bigcup M_i f\right\}. \quad (3)$$

According to this notation, the wavelet extrema representation of a signal f is defined as:

$$E_e f = \{M_a W_j f, M_i W_j f, M W_j f,\ j = 1, \cdots, J+1\}. \quad (4)$$

This means that $E_e f$ consists of indices of local extrema of $W_j f$ and the values of $W_j f$ at these points, and this for all scales $j = 1, 2, \cdots, J+1$.

The wavelet extrema representation contains information on both wavelet transform modulus maxima and minima. For a wavelet which is the first derivative of some smoothing function the maxima correspond to sharp variations in the signal while the minima occur at the points where the signal is maximally regular [2]. This does not necessarily lead to a significant increase in the number of points to be considered

with respect to the wavelet modulus maxima representation as would appear at first. It turns out that most of wavelet transform local extrema are actually modulus maxima (there are examples of signals for which the wavelet extrema and modulus maxima representations are the same). In experiments performed on lines from images and randomly generated signals we obtained that taking the modulus maxima instead of all local extrema reduces the total number of points by only about 10%. Another example of a convex modification of the original modulus maxima scheme is a representation which includes information on positions of local modulus minima without coding their values. Also, either the whole low-pass signal $W_{J+1}f$ or only its local extrema could be kept for this representation. For the sake of conciseness, in this paper, we will adhere to the definition (4) since most of the results apply to other cases as well.

The definition of wavelet zero-crossings representation requires the introduction of two more operators. Z will denote the operator which provides the zero-crossings of a sequence f:

$$Zf = \{k: f(k) \cdot f(k-1) \leq 0\}. \tag{5}$$

It is known that the zero-crossings by themselves do not provide a stable[1] characterization of signals [1]. Therefore the integral values of the function between zero-crossings are added in order to stabilize the representation [1]. Let S be the operator which gives the integral values (the sum of points) between all pairs of consecutive zero-crossings of some sequence. If the total number of zero-crossings of f is denoted by $|Zf|$, and its kth zero-crossing by z_k, the S operator is defined as:

$$Sf = \left\{ Sf(k): Sf(k) = \sum_{j=z_{k-1}}^{z_k - 1} f(j), k = 1, \cdots, |Zf| + 1 \right\}. \tag{6}$$

It is assumed here that the points $-\infty$ and $+\infty$ are also zero-crossings, denoted by z_0 and $z_{|Zf|+1}$, respectively. In order to ensure that $Sf(1)$ and $Sf(|Zf|+1)$ are finite, we shall require that the signal f be integrable, that is $f \in \ell^1(\mathbf{Z})$. Therefore, the following definition of wavelet zero-crossings representation is introduced for signals in $\ell^1(\mathbf{Z})$ (this is usually the case in practice, where signals with sufficient decay are encountered):

$$E_z f = \{ZW_j f, SW_j f,\ j = 1, \cdots, J+1\} \tag{7}$$

meaning that the zero-crossings representation, $E_z f$, consists of the indices of the zero-crossings of $W_j f$ and integral values of $W_j f$ between consecutive zero-crossings, across all scales $j = 1, 2, \cdots, J+1$.

In the last part of this section we consider mutual relationship between wavelet extrema and wavelet zero-crossings representations defined this way. Consider the extrema representation $R_e f$ of some signal $f \in \ell^2(\mathbf{Z})$,

$$R_e f = \{M_a f, M_i f, Mf\} \tag{8}$$

[1] By *stable* we mean that a small perturbation of the representation can not correspond to an arbitrarily large perturbation of the original signal.

and the zero-crossings representation $R_z \Delta f$ of its difference Δf,

$$\Delta f(n) = f(n+1) - f(n) \tag{9}$$

defined as

$$R_z \Delta f = \{Z\Delta f, S\Delta f\}. \tag{10}$$

According to the definitions of local extrema and zero-crossings, (1), (2), (5), the local extrema of f coincide with the zero-crossings of Δf:

$$M_a f \bigcup M_i f = Z\Delta f. \tag{11}$$

In addition to the equivalence between $M_a f \bigcup M_i f$ and $Z\Delta f$, Mf and $S\Delta f$ also provide equivalent information on the signal f. With z_k denoting the index (location) of the kth zero-crossing of Δf, $k = 1, 2, \cdots, |Z\Delta f|$, the following relations can be easily proven:

$$Mf = \{f(z_1), f(z_2), \cdots, f(z_{|Z\Delta f|})\} \tag{12}$$

$$S\Delta f = \{(f(z_1) - f(-\infty)), (f(z_2) - f(z_1)), \cdots, (f(+\infty) - f(z_{|Z\Delta f|}))\}. \tag{13}$$

Since in most practical cases $f(-\infty) = 0$ and $f(+\infty) = 0$, information contained in Mf and $S\Delta f$ are equivalent, i.e., one uniquely determines the other. We can now state the relation between the two representations as an immediate consequence of equalities (11), (12), (13), and the commutativity of the Δ and W_j operators.

Proposition 1: For signals in $\ell^2(\mathbf{Z})$, the wavelet extrema representation and the wavelet zero-crossings representation of the signal's first difference (9) provide an equivalent characterizations of the signal. Consider an arbitrary signal $f \in \ell^2(\mathbf{Z})$ and its difference Δf. Any signal in the reconstruction set of Δf, from its wavelet zero-crossings representation, is the first difference of some signal in the reconstruction set of f, from its wavelet extrema representation. Conversely, the first difference of any signal in the reconstruction set of f, from its wavelet extrema representation, is in the reconstruction set of Δf, from its wavelet zero-crossings representation.

III. Nonsubsampled Filter Banks for the Wavelet Transform

Discussions of nonsubsampled filter banks in this paper will be restricted to FIR filters and octave band trees implementing the wavelet transform, as illustrated by Fig. 1(a). For perfect reconstruction of an arbitrary signal $f \in \ell^2(\mathbf{Z})$ from its wavelet transform, $\mathbf{W}f$, it is necessary and sufficient that there exist two filters $G_0(z)$ and $G_1(z)$ satisfying

$$H_0(z)G_0(z) + H_1(z)G_1(z) = 1. \tag{14}$$

Then, an inverse of the wavelet transform operator $\mathbf{W}^{-1}$ can be implemented by a filter bank as shown in Fig. 1(b), which will be referred to as the nonsubsampled synthesis octave band filter bank. It can be shown that for stable reconstruction to

be plausible the filters $H_0(z)$ and $H_1(z)$ can not have any common zeros on the unit circle [8]. For the reconstruction scheme using only FIR filters following FIR analysis, perfect reconstruction condition (14) is equivalent to the constraint that $H_0(z)$ and $H_1(z)$ have no common zeros. These perfect reconstruction conditions are less restrictive than the one in critically sampled filter banks [9], and consequently allow a greater degree of freedom in choosing the prototype filters.

Note that the synthesis filters $G_0(z)$ and $G_1(z)$, and therefore the inverse wavelet transform operator, $\mathbf{W^{-1}}$, are not unique. An obvious solution for the reconstruction operator $\mathbf{W^{-1}}$ is represented by Fig. 1c, where $V(z)$ is

$$V(z) = V_1(z)V_1(z^{-1}) + V_2(z)V_2(z^{-1}) + \cdots + V_{J+1}(z)V_{J+1}(z^{-1}). \quad (15)$$

It amounts to filtering the octave band components $W_1 f, W_2 f, \cdots, W_{J+1} f$ by $U_1(z) = \tilde{V}_1(z)/V(z)$, $U_2(z) = \tilde{V}_2(z)/V(z)$, $\cdots$, $U_{J+1}(z) = \tilde{V}_{J+1}(z)/V(z)$ respectively, and adding the resulting sequences. This inverse is called the Hilbert adjoint of the dual operator of $\mathbf{W}$ [10], [8] and is denoted by $\tilde{\mathbf{W}}^*$. The reconstruction algorithms which we propose use iteratively the orthogonal projection operator onto the range of the wavelet transform $P_{\mathcal{V}}: \ell^2(\mathbf{I}) \rightarrow \ell^2(\mathbf{I})$, which is implemented as $P_{\mathcal{V}} = \mathbf{W}\tilde{\mathbf{W}}^*$. Note that only for $\mathbf{W^{-1}} = \tilde{\mathbf{W}}^*$ is the $P_{\mathcal{V}}$ operator: $P_{\mathcal{V}} = \mathbf{W}\mathbf{W^{-1}}$. Since the numerical complexity of the reconstruction algorithms depend on this operator it is desirable to implement it using FIR filters.

It is easy to see that the $\tilde{\mathbf{W}}^*$ operator has an FIR implementation if and only if $V(z)$ is equal to a constant or, without loss of generality, $V(z) = 1$. Note that $V(z)$ cannot be a delay, since it is a symmetric polynomial. Necessary and sufficient conditions for this to hold are given by the following proposition which is proven in Appendix A.

Proposition 2: $V(z)$ is equal to a constant if and only if

$$H_0(z)H_0(z^{-1}) + H_1(z)H_1(z^{-1}) = 1. \quad (16)$$

Filters satisfying condition (16) are called power complementary filters [11]. Proposition 2 immediately proves the following theorem.

Theorem 1: Consider the wavelet transform operator $\mathbf{W}$, implemented by an octave band nonsubsampled filter bank, with FIR analysis filters $H_0(z)$ and $H_1(z)$. $\tilde{\mathbf{W}}^*$, the Hilbert adjoint operator of the dual operator of $\mathbf{W}$, has an FIR implementation if and only if $H_0(z)$ and $H_1(z)$ are power complementary filters. In that case, $P_{\mathcal{V}} = \mathbf{W}\mathbf{W^{-1}}$ for $\mathbf{W^{-1}} = \tilde{\mathbf{W}}^*$, and $\tilde{\mathbf{W}}^*$ can be implemented by the nonsubsampled octave band synthesis filter bank (see Fig. 1(b)), with $G_0(z) = H_0(z^{-1})$ and $G_1(z) = H_1(z^{-1})$.

A subclass of all octave band nonsubsampled filter banks satisfying this requirement is the class of orthogonal FIR filter banks. In many signal processing tasks linear phase filters are desirable. However, the power complementary condition (16) excludes the possibility of nontrivial linear phase FIR designs [11]. Another feature relevant for wavelet transform extrema and zero-crossings schemes is the flatness of filters at zero and at half the sampling frequency. In the following we study design of power complementary filters with a given flatness at $z = 1$ and $z = -1$.

The flatness of a filter at some frequency is defined as the multiplicity of the root at that frequency of the first derivative of its frequency response. Maximally flat filters are filters having the first derivative of the frequency response with the maximum number of zeros on the unit circle. In applications of filter banks an important role is played by the regularity of the low-pass prototype filter, a feature which is closely related to the flatness of the filter at $\omega = \pi$ [10]. For example, in constructing orthonormal bases of wavelets from iterated filter banks, roughly speaking, a greater number of zeros of the low-pass filter at $\omega = \pi$ results in more regular wavelets. On the other hand, the number of vanishing moments of the wavelet obtained this way is determined by the multiplicity of zeros of the high-pass filter at $\omega = 0$.

The motivation behind wavelet extrema and wavelet zero-crossings representations is that for appropriately chosen wavelets, wavelet transform modulus maxima and zero-crossings occur at points of sharp variations of the signal [7]. An appropriate wavelet here means that it has to be the first derivative of some smoothing function in the modulus maxima case, or the second derivative of some smoothing function in the zero-crossings case. This implies that the prototype high-pass filter must have a zero of multiplicity one at $\omega = 0$ in the modulus maxima case, or multiplicity two in the zero-crossings case. The issue which we want to investigate here is how this affects the flatness of the low-pass filter. A constraint with the orthogonal filter bank design is that the low-pass prototype filter must have a zero of multiplicity one/two at $\omega = \pi$, in the extrema/zero-crossings case respectively, which means poor regularity, or poor smoothness of the wavelet. However, with general power complementary filters, zeros of the low-pass filter at $\omega = \pi$ are much less constrained.

The design procedure for maximally flat power complementary filters is given in Appendix B, as a constructive proof of Proposition 3, which states the main design result. Consider a pair of filters $H_0(z)$ and $H_1(z)$ satisfying the following conditions:

$$H_0(z)H_0(z^{-1}) + H_1(z)H_1(z^{-1}) = 1 \quad H_0(-1) = 0, \; H_1(1) = 0. \quad (17)$$

If the multiplicity of the zeros of $H_0(z)$ at $z = -1$ is N_0 and the multiplicity of the zeros of $H_1(z)$ at $z = 1$ is N_1, then the filters have flatness $N_0 - 1$ at $\omega = \pi$, and flatness $N_1 - 1$ at $\omega = 0$. In designing maximally flat filters, the issue is to maximize the flatness of the filters, i.e., to maximize $N_0 + N_1$ for the given filter length L. The following proposition holds.

Proposition 3: Consider a power complementary pair of filters $H_0(z)$ and $H_1(z)$ of length L, where $H_0(-1) = 0$ and $H_1(1) = 0$. Let N_0 be the multiplicity of the zeros of $H_0(z)$ at $\omega = \pi$, and N_1 be the multiplicity of the zeros of $H_1(z)$ at $\omega = 0$. It is possible to design $H_0(z)$ and $H_1(z)$ for any pair of N_0 and N_1 such that $1 \leq N_0 < L$, $1 \leq N_1 < L$, $N_0 + N_1 \leq L$.

A consequence is that in the design of power complementary filters for the wavelet extrema representation the low-pass filter can even be a binomial filter. In the zero-crossings case the low-pass filter of the power complementary pair can have all but one of its zeros at $\omega = \pi$. However, the low-pass filter does not necessarily have to be maximally flat in order to

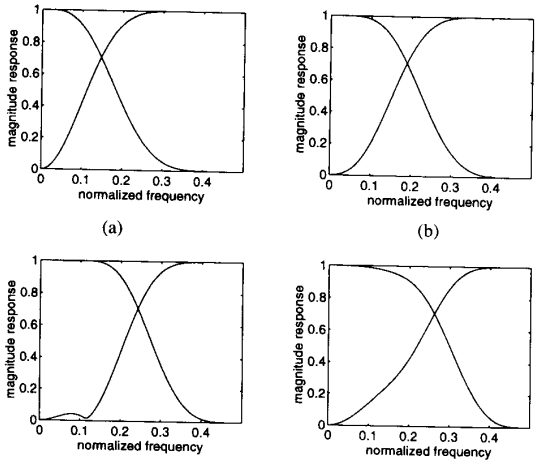

Fig. 2. Examples of power complementary filters for the wavelet zero-crossings representation. The length of the filters is $L = 9$, and the high-pass filters have a zero of multiplicity $N_1 = 2$ at $z = 1$ in all cases: (a) Maximally flat filters: low-pass filter has $N_0 = 7$ zeros at $z = -1$; (b) power complementary pair: low-pass filter with $N_0 = 6$ zeros at $z = -1$; (c) power complementary pair: low-pass filter with $N_0 = 5$ zeros at $z = -1$; (d) power complementary pair: low-pass filter with $N_0 = 4$ zeros at $z = -1$.

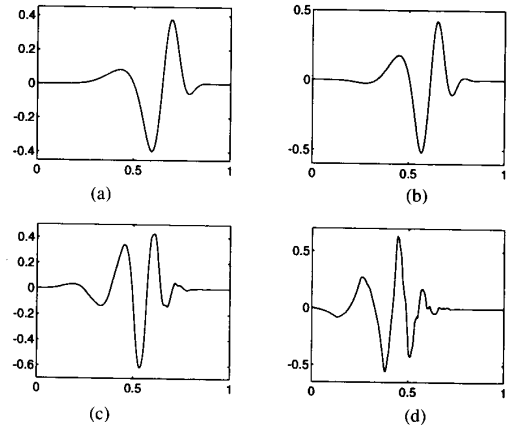

Fig. 3. Wavelets derived from the filters represented in Fig. 2. Wavelets in (a)–(d) are derived from filters in Fig. 2(a)–(d), respectively.

achieve sufficient regularity. This brings additional freedom which can be used to meet other design specifications. Fig. 2 illustrates several designs of power complementary filters for the wavelet zero-crossings representation with the parameter being the multiplicity of the zeros of the low-pass filter at $\omega = \pi$.

Wavelets for the wavelet extrema or zero-crossings representation can be generated using infinitely iterated octave band nonsubsampled filter banks. That is a standard procedure pioneered by Daubechies [16], and also discussed by Shensa in the nonsubsampled case. Details of this construction are given in Appendix C. Fig. 3 gives examples of wavelets derived from the power complementary filter banks represented in Fig. 2. It can be shown (see Appendix C) that wavelets derived from maximally flat power complementary filters of the length L are at least $L - 3$ times continuously differentiable in the extrema case, while in the zero-crossings case they are continuously differentiable at least $L - 3 - \frac{1}{2}\log_2 L$ times.

The connection between octave band filter banks and continuous-time multiresolution analysis was first pointed out by Mallat [13]. Mallat showed that in the case of critically sampled orthogonal filter banks, octave band trees can be used for efficient calculation of coefficients of wavelet expansions of continuous-time signals. That result is known as Mallat's algorithm. Recently, Shensa [14] showed that a similar relation between discrete and continuous-time frameworks exists in the case of nonsubsampled filter banks provided only that the perfect reconstruction condition (14) is satisfied. In Appendix D, we briefly state this relation and give a direct proof.

IV. Consistent Reconstruction

The wavelet extrema and zero-crossings representations of a signal represent a number of convex constraints which the signal obeys. In general, an infinite number of signals, which are signals in the reconstruction set, satisfy the same set of constraints. A consistent reconstruction strategy, which is our goal, means finding a signal in the reconstruction set since it satisfies all of the constraints and can not be distinguished from the original based on the representation. This notion is also important when quantization of extrema values (or integral values between zero crossings) is used, as would be the case in coding.

The reconstruction procedures described here actually recover from the representations the wavelet transform $F^* = \mathbf{W}f^*$ of a signal f^* in the reconstruction set, which is then itself obtained using the inverse wavelet transform. $\Phi_e^c(F)$, the closure of the reconstruction set of F from the local extrema of $W_j f$, $j = 1, \cdots, J+1$, can be represented as the intersection

$$\Phi_e^c(F) = \mathcal{V} \bigcap \mathcal{E} \bigcap \left(\bigcap_{i,j} \mathcal{C}_{i,j} \right) \tag{18}$$

of the following sets:

- $\mathcal{V}$—the range of the wavelet transform

$$\mathcal{V} = \{G : G = Wg \text{ for some } g \in \ell^2(\mathbf{Z})\}; \tag{19}$$

- $\mathcal{E}$—the set of all $G \in \ell^2(\mathbf{I})$, such that $G^i(k) = F^i(k)$ for all k which are local extrema of F^i, across all the scales $i = 1, 2, \cdots, J+1$;
- $\mathcal{C}_{i,j}$—the set determined by the requirement that the component G^i of $G \in \Phi_e^c(F)$ has to be nonincreasing/nondecreasing at the point j if F^i is decreasing/increasing at the same point. Note that the sets $\mathcal{C}_{i,j}$ are associated only to those points where F is strictly increasing or decreasing, i.e., only for those indices (i, j) such that $F^i(j) \neq F^i(j+1)$.

Obviously, $\mathcal{V}$ is a subspace of $\ell^2(\mathbf{I})$ and $\mathcal{E}$ and $\mathcal{C}_{i,j}$'s are closed convex sets, therefore alternating projections [15] of any initial point $F_0 \in \ell^2(\mathbf{I})$ onto $\mathcal{V}$, $\mathcal{E}$ and all the $\mathcal{C}_{i,j}$'s will converge to a point in their intersection, the reconstruction set $\Phi_e^c(F)$.

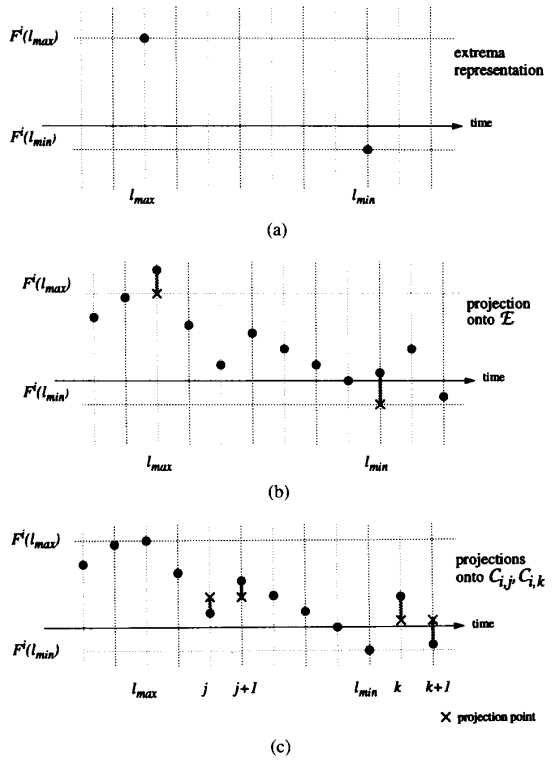

Fig. 4. Reconstruction from the wavelet extrema representation: implementations of projection operators: (a) Segment of the extrema representation of the sequence F^i, with the local maximum and minimum occurring at the points $l_{\max}$ and $l_{\min}$, respectively; (b) segment of the signal G^i (bold dots) and its projection onto $\mathcal{E}$ obtained by assigning it values of F^i at the points that are local extrema of F^i (crosses represent the new values of the altered points); (c) projection of G^i onto $\mathcal{E}$ is now represented by the bold dots. It is increasing at the point j and therefore is not in $C_{i,j}$. The projection is obtained by assigning points j and $j+1$ their arithmetic mean.

The projection $G_{\mathcal{E}}$ of some G onto $\mathcal{E}$ is obtained by assigning extrema values of F to the corresponding points of G (see Fig. 4(b)):

$$G^i_{\mathcal{E}}(k) = \begin{cases} F^i(k), & k \text{ is an extremum of } F^i \\ G^i(k), & \text{otherwise} \end{cases} \tag{20}$$

and $G_{C_{i,j}}$, the projection of some $G \in \ell^2(\mathbf{I})$ onto $C_{i,j}$, is equal to G, except possibly at the points j and $j+1$ of G^i, if the monotonicity condition imposed by the set $C_{i,j}$ is violated. In that case

$$G^i_{C_{i,j}}(k) = \begin{cases} \frac{1}{2}\cdot\left(G^i(j)+G^i(j+1)\right) & k = j, j+1 \\ G^i(k) & \text{otherwise} \end{cases} \tag{21}$$

as illustrated by Fig. 4(c).

Finding successive projections of some G onto $\mathcal{E}$ and all $C_{i,j}$'s consists of assigning the arithmetic mean to the pairs of points of G which do not obey the required monotonicity, and assigning the local extrema values of F at the corresponding points. This requires $O(JN)$ additions and $O(JN)$ divisions by two for a length N signal. The numerical complexity of the $P_{\mathcal{V}}$ operator is $O(JLN)$ additions and $O(JLN)$ multiplications, where L is the filters' length, provided that the conditions for an FIR implementation of $P_{\mathcal{V}}$ are met (see Section III).

In the wavelet zero-crossings case, the closure of the reconstruction set of $F = \mathbf{W}f$, from the wavelet zero-crossings representation of f, is the intersection

$$\Phi^c_z(F) = \mathcal{V} \bigcap \mathcal{U} \bigcap \left(\bigcap_{i,j} \mathcal{Z}_{i,j} \right), \tag{22}$$

where $\mathcal{U}$ and $\mathcal{Z}_{i,j}$ are defined as the following:

- $\mathcal{U}$—the set of all sequences $G \in \ell^2(\mathbf{I})$ such that for all scales $i = 1, \cdots, J+1$, F^i and G^i have the same integral values between any two adjacent zero-crossings of F^i. If z^i_k denotes the kth zero-crossing of F^i, then $\mathcal{U}$ can be written as:

$$\mathcal{U} = \left\{ \begin{matrix} G: G \in \ell^2(\mathbf{I}), \sum_{j=z^i_{k-1}}^{z^i_k - 1} G^i(j) = \sum_{j=z^i_{k-1}}^{z^i_k - 1} F^i(j) \\ k = 1, 2, \cdots, |ZF^i| + 1, i = 1, 2, \cdots, J+1 \end{matrix} \right\} \tag{23}$$

- $\mathcal{Z}_{i,j}$—the set of all sequences $G \in \ell^2(\mathbf{I})$ such that G^i has the same sign as F^i at point j. The $\mathcal{Z}_{i,j}$ sets are defined only for the nonzero points of F, only for those indices (i,j) satisfying $F^i(j) \neq 0$.

Since the sets $\mathcal{Z}_{i,j}$ and $\mathcal{U}$ are also closed and convex, a point in the reconstruction set $\Phi^c_z(F)$ can be reached as the limit of the sequence of alternating projections of an arbitrary starting point $F_0 \in \ell^2(\mathbf{I})$ onto $\mathcal{V}$, $\mathcal{U}$ and $\mathcal{Z}_{i,j}$'s. The projection $G_{\mathcal{Z}_{i,j}}$ of any vector $G \in \ell^2(\mathbf{I})$ onto $\mathcal{Z}_{i,j}$, is obtained by assigning a zero value to the point j of G^i if F^i and G^i don't have the same sign at that point, as shown in Fig. 5(a) and (b). The projection operator onto $\mathcal{U}$ operates on some G in the following way. All the sequences G^i of G are considered on intervals between consecutive zero-crossings of corresponding F^i's, and to each point of the interval the average difference of G^i and F^i on that interval is added (see Fig. 5(c)). Thus the projection $G_{\mathcal{U}}$ of a G onto $\mathcal{U}$ is given by

$$G^i_{\mathcal{U}}(k) = G^i(k) + \frac{1}{z^i_n - z^i_{n-1}} \sum_{j=z^i_{n-1}}^{z^i_n - 1} (F(j) - G(j)),$$
$$z^i_{n-1} \leq k < z^i_n,\ n = 1, \cdots, |ZF^i| + 1, i = 1, \cdots, J+1. \tag{24}$$

Thus, $G_{\mathcal{U}}$ has the same integral values as F on the intervals determined by the zero-crossings of F.

This algorithm actually iterates between operators $P_{\mathcal{V}}$, the projection operator onto $\mathcal{U}$, $P_{\mathcal{U}}$, and the projection operator onto $\mathcal{Z}$, $P_{\mathcal{Z}}$, where $\mathcal{Z}$ is the set of all vectors in $\ell^2(\mathbf{I})$ which have prespecified zero crossings. Numerical complexity of the composition of the projectors $P_{\mathcal{U}}$ and $P_{\mathcal{Z}}$ is $O(JN)$ additions and $O(JN)$ divisions by integers. A similar algorithm for consistent reconstruction from wavelet transform zero-crossings is proposed by Mallat [1]. Comparison between Mallat's algorithm and this algorithm is discussed in the next section.

It is important to note that in each iteration of the reconstruction algorithms the distance between the original signal and its estimate is decreased, which is a consequence of the fact that

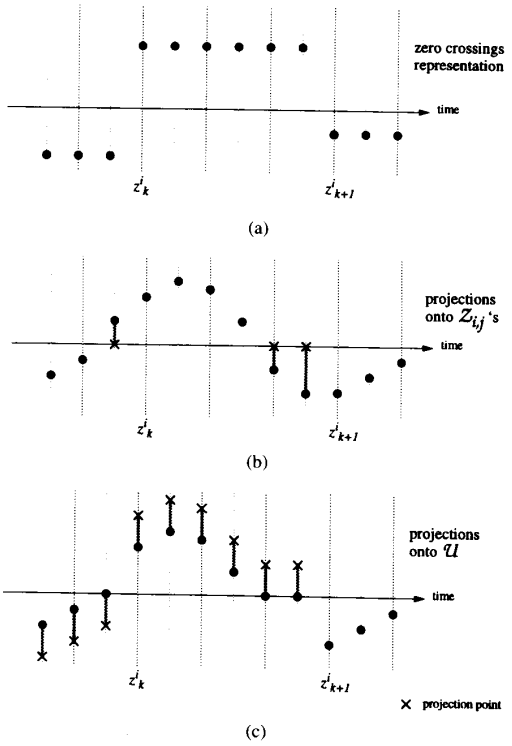

Fig. 5. Reconstruction from the wavelet zero-crossings representation: implementations of the projection operators: (a) Segment of the zero-crossings representation of F^i with zero crossings occurring at the points z_k^i and z_{k+1}^i; (b) segment of the sequence G^i represented by the bold dots. Its projections onto $\mathcal{Z}_{i,j}$'s are obtained by assigning zero values to those points that do not have the required sign; (c) projection of G^i onto $\mathcal{Z}_{i,j}$'s is represented by the dots. Its projection onto $\mathcal{U}$ is found by adding the same values to each point of the segments between zero crossings of F^i so that the required integral values are achieved.

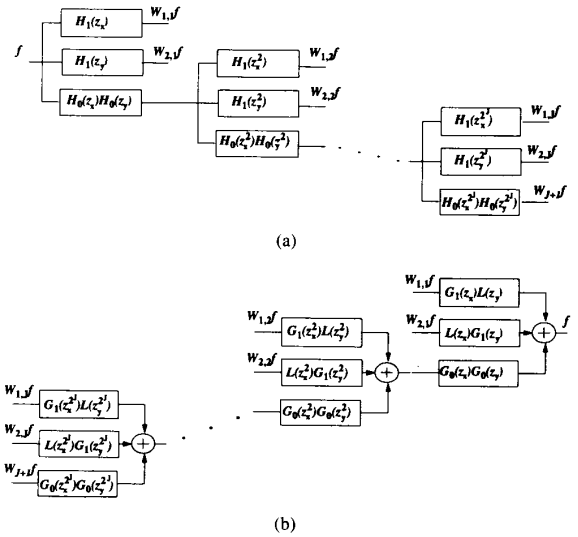

Fig. 6. Wavelet transform used in the 2-D wavelet zero-crossings representation: (a) Filter bank implementation of the 2-D wavelet transform operator $\mathbf{W}$; (b) filter bank implementation of an inverse of the 2-D wavelet transform operator.

projectors onto convex sets are nonexpansive operators. For alternative algorithms for consistent reconstruction, based on the gradient descent algorithm, the reader is referred to work by Berman *et al.* [3].

The discrete wavelet transform operator of two dimensional signals for wavelet modulus maxima [2], [7] and wavelet zero-crossings representations is the linear operator $\mathbf{W}: \ell^2(\mathbf{Z}^2) \rightarrow \ell^2(\{1,2,\cdots,2J+1\} \times \mathbf{Z}^2)$ consisting of $2J+1$ linear operators $W_{i,j}: \ell^2(\mathbf{Z}^2) \rightarrow \ell^2(\mathbf{Z}^2)$ $i = 1,2$ $j = 1,2,\cdots,J$ and $W_{J+1}: \ell^2(\mathbf{Z}^2) \rightarrow \ell^2(\mathbf{Z}^2)$. The operators $W_{1,j}$, $W_{2,j}$, and W_{J+1} denote respectively separable filtering with the filters

$$\begin{aligned} V_{1,j}(z_x, z_y) &= H_0(z_x)H_0(z_y)\cdots \\ &\quad \cdots H_0(z_x^{2^{j-1}})H_0(z_y^{2^{j-1}})H_1(z_x^{2^j}), \\ V_{2,j}(z_x, z_y) &= H_0(z_x)H_0(z_y)\cdots \\ &\quad \cdots H_0(z_x^{2^{j-1}})H_0(z_y^{2^{j-1}})H_1(z_y^{2^j}), \\ V_{J+1}(z_x, z_y) &= H_0(z_x)H_0(z_y)\cdots \\ &\quad \cdots H_0(z_x^{2^j})H_0(z_y^{2^j}). \end{aligned} \tag{25}$$

Defined this way, the wavelet transform operator $\mathbf{W}$ can be implemented using the filter bank based on the prototype filters $H_0(z)$ and $H_1(z)$ as shown in Fig. 6(a). Perfect reconstruction is possible provided that there exist two filters $G_0(z)$ and $G_1(z)$ satisfying (14). An inverse operator $\mathbf{W}^{-1}$ implemented again as a filter bank, based on the filters $G_0(z)$, $G_1(z)$ and $L(z) = \frac{1}{2}(1 + H_0(z)G_0(z))$, is illustrated by Fig. 6(b). For the analysis filters such that $H_0(z)$ is low-pass and $H_1(z)$ has exactly two zeros at $z = 1$, zero-crossings of $W_{1,j}f$s and $W_{2,j}f$s are related to multiscale sharp variations of f along x and y coordinates respectively. This explains the reasons for using this particular type of wavelet transform. For the details on this issue the reader is referred to the work by Mallat and Zhong [7].

The wavelet zero-crossings representation of two dimensional signals will be defined again using two operators, denoted as in the one dimensional case by Z and S, with similar meaning. The zero-crossings operator Z in $\ell^2(\mathbf{Z}^2)$ is defined as:

$$\begin{aligned} Zf = \{(k,l)&: f(k,l)f(k-1,l) \le 0 \\ &\text{or } f(k,l)f(k,l-1) \le 0\}. \end{aligned} \tag{26}$$

Zero-crossings of 2-D signals define a number of connected areas of points sharing the same sign, which are going to be referred to simply as *areas* in the following. The S operator, in the 2-D case, provides information on integral values (the sum of points) of the signal in each of these areas:

$$Sf = \left\{ \begin{matrix} Sf(k)\text{: the sum of points inside the area } k, \\ k = 1,2,\cdots, \text{ number of the areas} \end{matrix} \right\}. \tag{27}$$

Note that according to the definition (26) of zero-crossings, all the points of f where f assumes zero value, are declared as zero-crossings. In implementations these points can be associated with any of the contiguous areas. Analogously to the definition (7) in $\ell^2(\mathbf{Z})$, the wavelet zero-crossings representation for two-dimensional signals can be now defined

as

$$E_z f = \{ZW_{i,j}f, SW_{i,j}f, \\ i = 1,2\ j = 1,\cdots,J+1, ZW_{J+1}f, SW_{J+1}f\}. \quad (28)$$

The reconstruction algorithm from the wavelet zero-crossings representation of two-dimensional signals, defined in this manner, is a straightforward extension of the reconstruction algorithm in the case of signals in $\ell^2(\mathbf{Z})$, and details are not given here. However, it can be shown that for the wavelet transform for two-dimensional signals as defined in (25), the orthogonal projection operator onto the range of the wavelet transform can not have an FIR implementation. Instead, in experiments we used a $\mathbf{WW^{-1}}$ which has an FIR implementation. The FIR synthesis filters $G_0(z)$ and $G_1(z)$ are not unique and should be designed with a caution, because some choices may even lead to a divergence of the reconstruction algorithm. For instance, a pair of FIR synthesis filters which satisfy the perfect reconstruction condition can be obtained from $H_0(z)$ and $H_1(z)$ using Euclid's algorithm which gives a highpass filter $G_0(z)$ and a lowpass filter $G_1(z)$ for $H_0(z)$ and $H_1(z)$, which are lowpass and highpass, respectively. Such synthesis filters are certainly bad choice and in this case we observed divergence of the reconstruction algorithm. The design of synthesis filters which would insure convergence of the reconstruction algorithm in the case when $\mathbf{W^{-1}}$ is not implemented as the Hilbert adjoint of the dual of $\mathbf{W}$ is still an open problem. In experiments with power complementary filters $H_0(z)$ and $H_1(z)$ the reconstruction algorithm always converged for $G_0(z) = H_0(z^{-1})$ and $G_1(z) = H_1(z^{-1})$. In addition, we observed the convergence and very good reconstruction results for $G_0(z)$ and $G_1(z)$ whose magnitude responses were close to those of $H_0(z)$ and $H_1(z)$, respectively. Numerical complexity of the $\mathbf{WW^{-1}}$ operator is $O(JLN^2)$ additions and $O(JLN^2)$ multiplications if it is implemented using FIR filters of length L. The rest of the operators used in the reconstruction are analogous to their counter-parts in the one-dimensional case and their numerical complexity is $O(JN^2)$ additions and $O(JN^2)$ divisions by integers.

V. Experimental Results in Reconstruction of Signals from the Wavelet Extrema/Zero-Crossings Representation

Generally, signals can not be reconstructed with arbitrary high quality from their wavelet extrema/zero-crossings representations since the representations are nonunique. It can be shown that for finite length signals, the closures of the reconstruction sets are the convex hulls of finitely many vertices [3]. The sizes of the reconstruction sets, determined by the distances between these vertices, directly influence the quality of the reconstructed signal. Each wavelet transform extremum or zero-crossing represents a linear constraint which defines a hyperplane in the signal space bounding the reconstruction set. It can be expected that signals producing more extrema/zero-crossings have reconstruction sets of smaller sizes, and consequently yield better reconstruction results. However, the price paid is the larger number of points in the representation. Experiments generally confirm this rather heuristic argument. Signals with higher frequency content, which results in larger number of extrema or zero-crossings usually have faster convergence and better reconstruction.

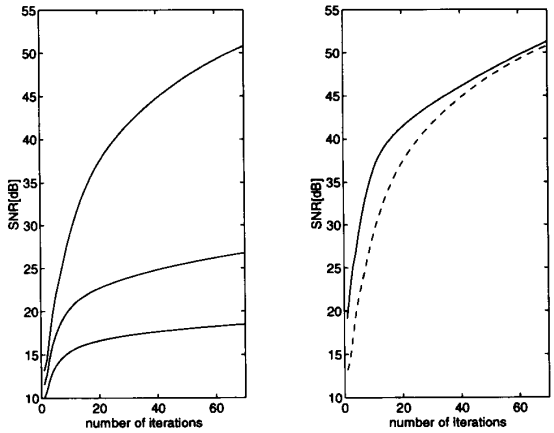

Fig. 7. Results of reconstruction of randomly generated 1-D signals: (a) SNR in the reconstruction from the wavelet zero-crossings representation obtained with wavelets having different regularities. Plots on the top, middle, and bottom correspond to wavelets on Fig. 2(c), (b), and (a), respectively; (b) SNR in the reconstruction from the wavelet extrema representation (solid line), and SNR in the reconstruction from the wavelet zero-crossings representation for the wavelet in Fig. 2(c) (dashed line).

Regularity of the wavelet used for the representation is of a paramount importance. The dyadic wavelet transform is a sequence of signals $f_{2^j} = \psi_{2^j} * f_c$, $j = 1,2,\cdots$, which are results of filtering an original signal $f_c \in L^2(\mathbf{R})$ by dilated versions of the wavelet ψ (see Appendix D). Obviously, in generating the component signals f_{2^j}, the original signal f_c and the dilated wavelets ψ_{2^j} play interchangeable roles. Therefore, the extrema or zero-crossings of the dyadic wavelet transform can result from the singularities of either the original signal or the wavelet. If the aim is to suppress those local extrema/zero-crossings which are rather wavelet than signal related it is advisable to use smoother wavelets. However, more regular wavelets generally produce reduced number of wavelet transform extrema/zero-crossings, and consequently yield poorer reconstruction results. As an illustration of the above discussion, Fig. 7(a) represents results in reconstruction of randomly generated signals from the wavelet transform zero-crossings for wavelets with different regularity properties. Experimental results in the reconstruction from wavelet extrema representation are represented in Fig. 7(b). For a comparison with the zero-crossings reconstruction, one of the curves from Fig. 7(a) is plotted again on the same graph. Note that in both cases shown in Fig. 7(b), the plots represent an average for the same set of random signals, and that the total number of the zero-crossings was on average around 6.5% smaller than the number of the extrema. In the experiments with wavelet transform extrema representation, we used the same filters as Mallat *et al.* for their wavelet modulus maxima scheme [7].

There is a difference between Mallat's algorithm for reconstruction from wavelet transform zero-crossings [1] and the algorithm presented here. As stated in the previous section, the new algorithm iterates between $P_{\mathcal{V}}$, $P_{\mathcal{U}}$ and $P_{\mathcal{Z}}$, while Mallat's algorithm iterates between $P_{\mathcal{V}}$ and the projection operator onto $\Gamma = \mathcal{U} \bigcap \mathcal{Z}$, P_Γ. Numerical complexity of P_Γ is $O(JN \log N)$ additions and $O(JN)$ divisions by integers. On the other hand the composition of $P_{\mathcal{Z}}$ and $P_{\mathcal{U}}$ requires $O(JN)$ additions and $O(JN)$ divisions by integers and reduced number of loops with respect to P_Γ. It may appear that the new algorithm has a slower convergence since the constraints in Γ are split between $\mathcal{U}$ and $\mathcal{Z}$, and successive projections onto $\mathcal{U}$ and $\mathcal{Z}$ in general do not yield projection onto Γ. However, the situation is not so simple. It is possible to come up with examples where such splitting strategy can even improve speed of convergence or give exactly the same results at a reduced cost of implementation. For instance, if we start the reconstruction with a point inside Γ and the reconstructed signals stayed in $\mathcal{Z}$ throughout the reconstruction procedure, the two algorithms would give the same result. Experiments showed that during the reconstruction process all intermediate solutions are very close to $\mathcal{Z}$, if not inside it, and hence that the composition of operators $P_{\mathcal{U}}$ and $P_{\mathcal{Z}}$ yields points close to those obtained by the P_Γ operator. In most cases we observed that the reconstructed signals obtained by Mallat's and the new algorithm, starting at a same point, were very close and differed in the reconstruction error typically by less than 0.1 dB in each iteration.

Examples of images reconstructed from wavelet zero-crossings representations are shown in Fig. 8. The size of the originals (the left column) is 256 × 256 pixels, and the reconstructed images (the right column) are obtained after 10 iterations of the algorithm. In these experiments the wavelet transform is performed across four scales and the representation included the whole signal $W_{J+1}f$ (there is no significant difference in the reconstruction error with respect to the case when only zero-crossings information on $W_{J+1}f$ is used). As in the case of one-dimensional signals we observed that using more regular filters reduces the amount of data to be recorded but increases the mean-squared reconstruction error. In all experiments with images, reported here, we used linear phase filters: $H_0 = \frac{1}{4}[1\ 2\ 1]$, $H_1 = \frac{1}{4}[1\ -\ 2\ 1]$, $G_0 = \frac{1}{8}[-\ 1\ 2\ 6\ 2\ -\ 1]$, and $G_1 = \frac{1}{8}[1\ 2\ -\ 6\ 2\ 1]$.

Some modified versions of the original wavelet zero-crossings scheme can be more convenient. The definition of the two dimensional wavelet zero-crossings representation, as introduced in the preceding section, can be generalized in the following manner. Some of the areas of the same sign can be partitioned into several subareas, and information on these subareas, locations and integral values, extracted separately. This increases the overhead, but generally decreases distortion of the representation and may facilitate some signal processing tasks, such as the selection of important edges. On the other hand, only partial information on the wavelet transform zero-crossings can be kept, which has the opposite effect on rate-distortion properties of the scheme. The reconstruction algorithm can be modified in a straightforward manner to accommodate these variants of the representation. Fig. 9 illustrates the reconstruction of an image from the representation obtained by combining the two general approaches. Black regions in the two-level images represent the subareas which are included in the representation, across four scales of the wavelet transform. The selected subareas are those with positive integral values and average intensity above a given threshold. The original (bottom left) is the 256 × 256 image, and the reconstructed signal (bottom right) is obtained after 10 iterations of the algorithm, with 20.8 dB SNR.

The number of subareas used in the representation is 5146. It can be noticed that even with this rather naive selection process, wavelet zero-crossings representation provides the information on important multiscale edges and yields good reconstruction.

VI. Conclusion

The wavelet extrema and zero-crossings representations were considered in discrete time using filter banks tools. We investigated relevant properties and design of the nonsubsampled filter banks which implement the wavelet transform for the representations. The relation between the two representations was established, showing that the wavelet extrema representation and the wavelet zero-crossings representation of the first difference yield equivalent characterizations of signals. The new understanding of the structures of the reconstruction sets, introduced here, turns out to be convenient for devising simple and efficient reconstruction procedures. Besides consistency in the reconstruction, and low numerical complexity, these algorithms are simple and easy to implement. The wavelet transform zero-crossings representation of two dimensional signals was also discussed as a multiscale edge representation. The results of this paper were presented in the wavelet transform framework, but it should be emphasized that most of them hold for arbitrary invertible overcomplete linear transforms.

Appendix A

Sufficiency is obvious from the definition of $V(z)$. Necessity is to be proven next. It can be deduced from (15), and the definitions of the filters $V_j(z)$, that the filters $H_0(z)$ and $H_1(z)$ must have equal lengths, because otherwise one of the factors $V_J(z)V_J(z^{-1})$ or $V_{J+1}(z)V_{J+1}(z^{-1})$ in $V(z)$ would contain powers of z and z^{-1} of higher order than any other factors in $V(z)$ of (15), and therefore $V(z) = const$ could not be achieved. Furthermore, if $H_0(z)H_0(z^{-1}) + H_1(z)H_1(z^{-1})$ contained any nonzero power of z, $V_{J+1}(z)V_{J+1}(z^{-1})$, and $V_J(z)V_J(z^{-1})$ in $V(z)$ would add to a polynomial having powers of z and z^{-1} of higher order than any other factor in the sum (15), and consequently the possibility of $V(z) = const$ would be lost. Hence, it is necessary that $H_0(z)H_0(z^{-1}) + H_1(z)H_1(z^{-1}) = k$, and it can easily be seen that k must be equal to 1.

Appendix B

The design procedure described here follows along the same lines as the design of maximally flat orthogonal filter banks

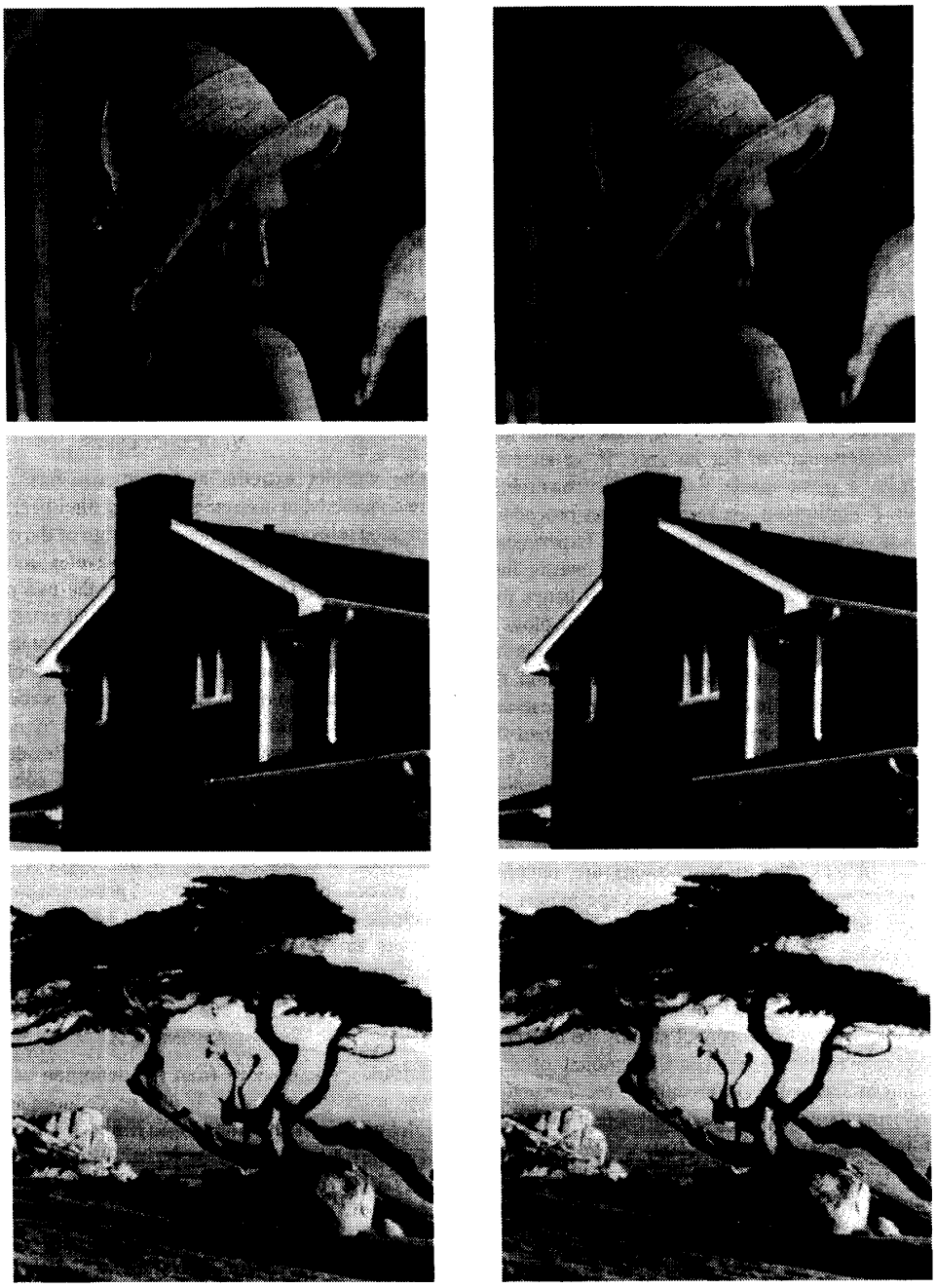

Fig. 8. Examples of images reconstructed from the wavelet zero-crossings representation. Left column: the originals, 256 × 256 pixels. Right column: reconstructed images, obtained after 10 iterations of the algorithm. SNR's are 36.1, 40.3, and 33.6 dB for "Lenna," "House," and "Tree" images, respectively.

[10], [11]. There is a bijective mapping between the set of FIR autocorrelation functions with real coefficients and the set of polynomials over $\mathbf{R}$ which are positive on the interval [0, 1]. The autocorrelation function $H(z)H(z^{-1})$ of a real FIR filter defines a real coefficient polynomial of $\sin^2 \frac{\omega}{2}$ on the unit circle:

$$H(e^{j\omega})H(e^{-j\omega}) = P\left(\sin^2 \frac{\omega}{2}\right). \tag{29}$$

On the other hand, any polynomial $P(y)$, positive on [0, 1], with $y = (\frac{1-z}{2})(\frac{1-z^{-1}}{2})$ defines an FIR autocorrelation function

$$P\left(\left(\frac{1-z}{2}\right)\left(\frac{1-z^{-1}}{2}\right)\right) = H(z)H(z^{-1}). \tag{30}$$

According to this, in order to obtain power complementary filters of length L having flatness of order $N_0 - 1$ at $\omega = \pi$

Fig. 9. The "Lenna" image reconstructed from partial wavelet zero-crossings representation. Bottom left: 256 × 256 original. Bottom right: the image obtained after 10 iterations of the reconstruction algorithm, with 20.8 dB SNR (PSNR is 28.0 dB). Bilevel images: black regions mark selected areas across four scales of the wavelet transform; the number of selected areas is 5146. Top left, top right, middle left, and middle right images represent scales 1, 2, 3, and 4, respectively.

and flatness $N_1 - 1$ at $\omega = 0$, it is sufficient to find

$$P(y) = (1 - y)^{N_0} Q(y) \tag{31}$$

such that $Q(y)$ has no zeros at $y = 1$, and $P'(y)$, the formal derivative of $P(y)$, has a zero of multiplicity $N_1 - 1$ at $y = 0$.

For the case of maximally flat filters, the coefficients of the polynomial

$$Q(y) = \sum_{l=0}^{L-1-N_0} q_l y^l \tag{32}$$

are obtained from the requirement that $P'(y)$ has a (N_1-1)th order zero at $y=0$ and that $P(0)=1$. This gives

$$q_l = \binom{N_0+l-1}{l},\ l=0,1,\cdots,L-1-N_0. \tag{33}$$

$H_0(z)$ is then obtained from (30), while $H_1(z)$ is derived by factoring

$$1-P\left(\left(\frac{1-z}{2}\right)\left(\frac{1-z^{-1}}{2}\right)\right) \tag{34}$$

as $H_1(z)H_1(z^{-1})$. That this is always possible to do is ensured by the fact that $P(y)$ has all of its extrema at $y=0$ and $y=1$, and therefore it is monotonically decreasing from 1 to 0 on the interval $[0,1]$, which makes expression (34) being positive on the unit circle. This gives the class of maximally flat power complementary filters.

In the case of the filters which are not maximally flat, $N_0+N_1<L$, $P(y)$ still has the form $(1-y)^{N_0}Q(y)$, and the coefficients $q_l, l=0,1,\cdots,N_1-1$, are determined as in (33). This gives the required flatness of the filters. The rest of coefficients of $Q(y)$ represent additional degrees of design freedom.

Appendix C

The derivation of wavelets from the iterated filter banks is as follows. Consider an octave band nonsubsampled filter bank of depth i and equivalent filters of the two lowest branches

$$H_0^{(i)}(z) = \prod_{k=0}^{i-1} H_0(z^{2^k}), \tag{35}$$

$$H_1^{(i)}(z) = H_1(z^{2^{i-1}}) \prod_{k=0}^{i-2} H_0(z^{2^k}). \tag{36}$$

Note that $H_0(z)$ and $H_1(z)$ denote the prototype low-pass and high-pass filters, respectively. Then associate with the impulse responses $h_0^{(i)}$ and $h_1^{(i)}$ of $H_0^{(i)}(z)$ and $H_1^{(i)}(z)$ the continuous time functions $\phi^{(i)}(x)$ and $\psi^{(i)}(x)$:

$$\phi^{(i)}(x) = 2^i h_0^{(i)}(n),\ \frac{n}{2^i} \le x < \frac{n+1}{2^i}, \tag{37}$$

$$\psi^{(i)}(x) = 2^i h_1^{(i)}(n),\ \frac{n}{2^i} \le x < \frac{n+1}{2^i}. \tag{38}$$

The elementary interval is divided by 2^i so that the continuous time functions remain compactly supported as $i \to \infty$. The factor 2^i which multiplies $h_0^{(i)}$ and $h_1^{(i)}$ is needed in order to maintain the L^2 norms of the associated continuous-time functions inside finite bounds[2]. Assume that $\phi^{(i)}(x)$ and $\psi^{(i)}(x)$ converge in the L^2 sense to the limits[3]:

$$\phi(x) = \lim_{i\to\infty} \phi^{(i)}(x), \tag{39}$$

$$\psi(x) = \lim_{i\to\infty} \psi^{(i)}(x). \tag{40}$$

[2]Note that in the case of the construction of wavelets from critically sampled filter banks this renormalization factor is $2^{\frac{i}{2}}$.

[3]For an in depth review of the conditions which ensure this convergence the reader is referred to [10].

Functions $\phi(x)$ and $\psi(x)$ obtained as the limits of the above construction are the scaling function and the wavelet derived from this filter bank.

Regularity of the derived wavelets can be estimated using Daubechies' criterion [10], [16]. According to that criterion, wavelet derived from a filter bank with the low-pass filter

$$H_0(e^{j\omega}) = \left(\frac{1+e^{j\omega}}{2}\right)^{N_0} R(\omega) \tag{41}$$

is r times continuously differentiable if

$$B = \sup_{\omega\in[0,2\pi]}|R(\omega)| < 2^{N_0-r-1}. \tag{42}$$

For the maximally flat power complementary filter design, described in the previous appendix

$$B = \sup_{y\in[0,1]}\sqrt{Q(y)} \tag{43}$$

where $Q(y)$ is the polynomial defined in (31), while its coefficients are given by (33). In the case of filters for wavelet extrema representation of length L, $Q(y)\equiv 1$ and $N_0 = L-1$, which implies that the derived wavelet is at least $L-3$ times continuously differentiable. In the zero-crossings case, the low-pass filter has all but one of its zeros at $\omega=\pi$, and therefore from (31) and (33) it follows that $N_0 = L-2$, while $Q(y) = 1+(L-2)y$. Consequently $B=\sqrt{L-1}$ and Daubechies' criterion immediately proves that the derived wavelet is at least $L-3-\frac{1}{2}\log_2 L$ times continuously differentiable.

Appendix D

Consider an octave band nonsubsampled filter bank with the prototype filters $H_0(z)$ and $H_1(z)$. Assume that this filter bank is regular, i.e., that continuous-time functions $\phi^{(i)}(x)$ and $\psi^{(i)}(x)$ associated to this filter bank in the manner described in the above appendix converge to $\phi(x)$ and $\psi(x)$ in the L^2 sense. In Fourier domain the scaling function $\phi(x)$ and the wavelet $\psi(x)$ derived in this way are given by

$$\hat{\phi}(\omega) = \prod_{k=1}^{\infty} H_0(e^{j2^{-k}\omega}), \tag{44}$$

$$\hat{\psi}(\omega) = H_1(e^{j2^{-1}\omega}) \prod_{k=2}^{\infty} H_0(e^{j2^{-k}\omega}). \tag{45}$$

For an arbitrary continuous-time signal $f_c(x)\in L^2(\mathbf{R})$, let the input of the filter bank be the sequence of samples of $f_c(x)$ smoothed by $\phi(x)$. Then the filter bank produces sequences of samples of the dyadic wavelet transform [7] of $f_c(x)$. That is, if $f\in\ell^2(\mathbf{Z})$ denotes the sampled version of $\phi * f_c$,

$$f(n) = \phi * f_c(n) \tag{46}$$

the output of the filter bank is

$$W_j f(n) = \psi_{2^j} * f_c(n)\ j=1,2,\ldots. \tag{47}$$

where $\psi_{2^j}(x) = \frac{1}{2^j}\psi(\frac{x}{2^j})$.

The relation (47) can be proven as follows. The discrete-time signal f in (46) is given in the Fourier domain as

$$\hat{f}(e^{j\omega}) = \sum_{k=-\infty}^{+\infty} \hat{f}_c(\omega+2k\pi)\hat{\phi}(\omega+2k\pi).$$

Then

$$W_l f(n) = \frac{1}{2\pi}\int_{-\pi}^{\pi} V_l(e^{j\omega})\cdot \cdot\left(\sum_{k=-\infty}^{+\infty}\hat{f}_c(\omega+2k\pi)\hat{\phi}(\omega+2k\pi)\right)e^{j\omega n}d\omega = \frac{1}{2\pi}\int_{-\infty}^{+\infty} V_l(e^{j\omega})\hat{f}_c(\omega)\hat{\phi}(\omega)e^{j\omega n}d\omega.$$

According to the definitions of $\hat{\phi}(\omega)$ and $\hat{\psi}(\omega)$ in (44) and (45), it follows that $\hat{\phi}(\omega)V_l(e^{j\omega}) = \hat{\psi}(2^l\omega)$, and therefore

$$W_l f(n) = \frac{1}{2\pi}\int_{-\infty}^{+\infty}\hat{f}_c(\omega)\hat{\psi}(2^l\omega)e^{j\omega n}d\omega,$$

which immediately gives relation (47).

ACKNOWLEDGMENT

The authors would like to express our gratitude to Prof. N. Thao for fruitful discussions on the topic, Prof. S. Mallat for his insightful comments on this paper, Dr. M. Unser for suggesting the introduction of the 2-D wavelet zero-crossings representation, and D. Lee for writing the software we used in the experiments. They are also grateful to reviewers for their constructive suggestions that improved the final manuscript.

REFERENCES

[1] S. Mallat, "Zero crossings of a wavelet transform," *IEEE Trans. Inform. Theory*, vol. 37, pp. 1019–1033, July 1991.
[2] S. Mallat and W. L. Hwang, "Singularity detection and processing with wavelets," *IEEE Trans. Inform. Theory*, vol. 38, pp. 617–643, Mar. 1992.
[3] Z. Berman and J. S. Baras, "Properties of the multiscale maxima and zero-crossings representations," *IEEE Trans. Signal Processing*,, vol. 41, pp. 3216–3231, Dec. 1993.
[4] Z. Berman, "Generalization and properties of the multiscale-maxima and zero-crossings representations," Ph. D. dissertation, Univ. of Maryland, College Park, 1992.
[5] Y. Meyer, "Un contre-exemple à la conjecture de Marr et à celle de S. Mallat," preprint, 1991.
[6] N. T. Thao and M. Vetterli, "Deterministic analysis of oversampled A/D conversion and decoding improvement based on consistent estimates," *IEEE Trans. Signal Processing*, vol. 42, pp. 519–531, Mar. 1994.
[7] S. Mallat and S. Zhong, "Characterization of signals from multiscale edges," *IEEE Trans. Pattern Anal. Machine Intell.*, vol. 14, pp. 710–732, July 1992.
[8] Z. Cvetković and M. Vetterli, "Non-subsampled filter banks: Frames for $\ell^2(\mathbf{Z})$ and continuous time signal processing," Tech. Rep. CU/CTR/TR 352-93-32, Columbia Univ., Dec. 1993.
[9] M. Vetterli and C. Herley, "Wavelets and filter banks: Theory and design," *IEEE Trans. Signal Processing*, vol. 40, pp. 2207–2232, Sept. 1992.
[10] I. Daubechies, "Ten lectures on wavelets," *CBMS-NSF Series in Appl. Math*, SIAM, 1992.
[11] P. P. Vaidyanathan, *Multirate Systems and Filter Banks*. Englewood Cliffs, NJ: Prentice-Hall, 1993.
[12] S. Mallat, "Multiresolution approximation and wavelet orthonormal bases of L^2," *Trans. Amer. Math. Soc.*, vol. 315, pp. 69–87, Sept. 1987.
[13] ——, "A Theory of multiresolution signal decomposition: The wavelet transform," *IEEE Trans. Pattern Anal. Machine Intell.*, vol. 11, pp. 674–693, July 1989.
[14] M. J. Shensa, "The discrete wavelet transform: Wedding the À Trous and Mallat algorithms," *IEEE Trans. Signal Processing*, vol. 40, pp. 2464–2482, Oct. 1992.
[15] D. C. Youla, "Mathematical theory of image restoration by the method of convex projections," in *Image Recovery—Theory and Application*. New York: Academic, 1987.
[16] I. Daubechies, "Orthonormal bases of compactly supported wavelets," *Commun. Pure Applied Math.*, vol. 41, pp. 909–996, Nov. 1988.

Zoran Cvetković received the Dipl. Ing. El. and Mag. El. degrees from the School of Electrical Engineering, University of Belgrade, Yugoslavia, in 1989, and 1992, respectively. Currently, he is pursuing the Ph.D. degree at the Department of Electrical Engineering and Computer Science at the University of California at Berkeley.

During the period 1989–1991, he worked as a Research and Teaching Assistant at the University of Belgrade. During the period from 1992 to 1993, he was a Graduate Research Assistant at Columbia University. In the summer of 1994, he worked for the Keck Center for Integrative Neuroscience, University of California at San Francisco, San Francisco, CA. His research interests include Weyl–Heisenberg wavelet frames, multirate signal processing, and modeling of the auditory system

Martin Vetterli (SM'90) received the Dipl. El.-Ing. degree from ETH Zürich, Switzerland, in 1981, the M.S. degree from Stanford University in 1982, and the Doctorat és Science degree from EPF Lausanne, Switzerland, in 1986.

He was a Research Assistant at Stanford and EPFL and has worked for Siemens and AT&T Bell Laboratories. In 1986, he joined Columbia University, New York, NY, where he is currently Associate Professor of Electrical Engineering. Since July 1993, he has also been on the faculty of the Department of Electrical Engineering and Computer Science at the University of California, Berkeley. His research interests include wavelets, multirate signal processing, computational complexity, signal processing for telecommunications, and digital video processing and compression.

Dr. Vetterli is a member of SIAM and ACM and of the editorial boards of *Signal Processing, Image Communication, Annals of Telecommunications Applied and Computational Harmonic Analysis*, and *The Journal of Fourier Analysis and Applications*. He received the Best Paper Award of EURASIP in 1984 for his paper on multidimensional subband coding, the Research Prize of the Brown Bovery Corporation (Switzerland) in 1986 for his thesis, and the IEEE Signal Processing Society's 1991 Senior Award for a 1989 Transactions paper with D. LeGall. He was a plenary speaker at the *1992 IEEE ICASSP* and is coauthor, with J. Kovacević, of the forthcoming book *Wavelets and Subband Coding* (Englewood Cliffs, NJ: Prentice-Hall, 1994).